**ULTRACARBONACEOUS ANTARCTIC MICROMETEORITES (UCAMMS): CLUES FOR THEIR ORIGIN.** C. Engrand[1], E. Charon[1,2], J. Duprat[1], E. Dartois[3], H. Leroux[4], K. Benzerara[5], C. Le Guillou[4], S. Bernard[5], S. Swaraj[6], R. Belkhou[6], L. Delauche[1], M. Godard[1], B. Augé[1].[1]CSNSM CNRS/Univ. Paris Sud, Université Paris-Saclay, 91405 Orsay Campus, France (cecile.engrand@csnsm.in2p3.fr), [2]now at NIMBE, CEA, CNRS, Université Paris-Saclay, CEA Saclay 91191 Gif-sur-Yvette France, [3]ISMO CNRS/Univ. Paris Sud, Université Paris-Saclay, 91400 Orsay Campus, France. [4]UMET Univ. Lille 1, 59650 Villeneuve d'Ascq, France, [5]IMPMC, 4 place Jussieu, 75005 Paris, France. [6]Synchrotron SOLEIL, HERMES Beamline, Saclay St Aubin, France.

**Introduction:** Ultracarbonaceous Antarctic Micrometeorites (UCAMMs) are identified in the Dome Fuji and JARE micrometeorite collections [1-3], and in the Dome C Concordia collection [4, 5]. These micrometeorites are dominated by organic matter containing minerals inclusions. At least two types of organic matter co-exist in varying proportion in UCAMMs, mostly distinguished by their N content. We present a first summary of the properties of a significant number of UCAMMs in order to better constrain their origin and formation processes.

**Samples and methods:** Sixteen UCAMMs have been identified in the Concordia collection so far, based on SEM/EDX of one UCAMM fragment (Table 1). Synchrotron-based Fourier transform infrared (FTIR) microscopy was acquired on a complementary fragment for twelve of them. The composition of ten of these UCAMMs (including C, N, O) was measured by electron microprobe analysis (EMPA) using dedicated standards at the CAMPARIS facility (Paris). Detailed mineralogical description was made by transmission electron microscopy (TEM) at UMET (Lille) for 3 UCAMMs [6]. STXM analyses were acquired for 4 UCAMMs at the ALS Berkeley facility and SOLEIL HERMES beamlines, with associated TEM at UMET [7, 8]. NanoSIMS analyses were performed at MNHN Paris and Institut Curie Orsay [5, 9, 10]. UCAMMs were also used as analogues for the preparation of Rosetta/COSIMA analyses by ToF-SIMS [11, 12].

| Name | initial size (µm)* | | Analyses performed | Refs |
|---|---|---|---|---|
| DC021119 | 87 | 110 | SEM, IR, Raman, EMPA | [15] |
| DC020940 | 42 | 82 | SEM | - |
| DC020941 | 40 | 72 | SEM, TEM | [6] |
| DC0609119 | 108 | 275 | SEM, IR, Raman, EMPA, NanoSIMS | [5,13,15] |
| DC0604139 | 50 | 90 | SEM | - |
| DC060718 | 53 | 87 | SEM, IR, Raman, EMPA, TEM, STXM/XANES | [7,15] |
| DC060919 | 50 | 79 | SEM, IR, Raman, EMPA, TEM, NanoSIMS | [5,6,13,15] |
| DC0611308 | 65 | 91 | SEM | - |
| DC060741 | 80 | 200 | SEM, IR, Raman, EMPA, TEM, STXM/XANES | [8,15] |
| DC060443 | 24 | 28 | SEM, IR, Raman, EMPA, TEM, STXM/XANES | [8,15] |
| DC060945 | 42 | 83 | SEM, IR, Raman, TEM | [6,13] |
| DC060565 | 33 | 44 | SEM, IR, Raman, EMPA, NanoSIMS, STXM/XANES | [9,10,14,15] |
| DC060594 | 53 | 66 | SEM, IR, Raman, EMPA, TEM, ToF-SIMS, NanoSIMS | [9,10,11,12,14,15,24] |
| DC142153 | 40 | 90 | SEM, IR, Raman, EMPA | - |
| DC161130 | 150 | 150 | SEM, IR, Raman, EMPA | - |
| DC1614309 | 60 | 70 | SEM, IR, Raman | - |

*Min-max dimensions

**Table 1**. List of the Concordia UCAMMs identified so far, with analytical techniques used and associated references.

**Results and discussion:**

UCAMMs of this work are found in all collections performed at Dome C in 2002, 2006, 2014, and 2016. Their relative proportion is ~ 1% of all analyzed particles. They are dominated by a polyaromatic globally N-rich organic matter [13-15], that shows bulk D enrichments, and heterogeneous distributions of the D/H and $^{15}N/^{14}N$ isotopic ratios [5, 9, 10]. STXM-XANES measurements of UCAMMs have shown that several organic phases are present, with different N contents [2, 7, 8, 16, 17]. Electron microprobe analyses performed in this work show a bimodal distribution of the N/C ratios from low values to ~ 0.20, with 2 clustering values around N/C ~ 0.05 and 0.18, respectively (Fig. 1). The values for N/C ~ 0.05 are on the upper limit of the values measured in insoluble organic matter (IOM) extracted from carbonaceous chondrites (CCs), whereas values > 0.10 are likely to be above the N/C of carbonaceous dust in the ISM (see [15]). The average C/Si atomic ratio of each UCAMM exhibits a large range of variations from ~11 to > 1000 (Fig. 2 top), well above both solar and ISM values (see [15]).

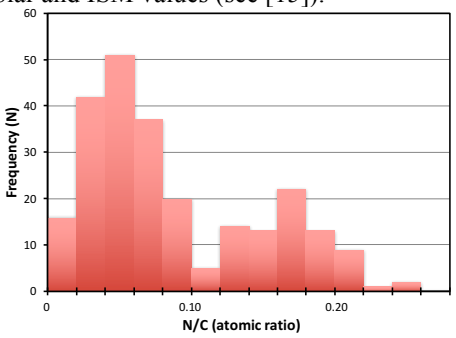


**Figure 1**: Frequency distribution of N/C measured by EMPA on a series of 10 UCAMMs previously analyzed by FTIR microscopy (4 to 45 independent locations were analyzed for each UCAMM).

By contrast, the range of variation of O/Si ratio in UCAMMs (Fig. 2 bottom) is compatible with the solar value. There is a clear correlation in the EMPA data between O and Si abundances, indicating that, when silicates are present, most of the O is carried by the silicates (Fig. 3). This observation corroborates the fact that the UCAMM organic matter generally carries lower O abundance than found in IOM, as observed by FTIR microscopy [14, 15]. The mineralogy of UCAMMs is usually dominated by low-Ca pyroxenes, olivine, Fe sulfides, and GEMS (Glass embedded with Metals and Sulfides) (see also [2, 3, 6]). In Concordia UCAMMs, the GEMS compositions are comparable

with that of GEMS in IDPs (Fig. 4). The abundance of pyroxene relative to olivine is higher in UCAMMs (and in AMMs in general) than in CCs. This might reflect a preferential alteration of the pyroxenes in the CCs, or a mineralogical zoning in the early protoplanetary disk (e.g. [18, 19]). GEMS are fragile phases, tracing potential alteration processes. In UCAMMs, most GEMS seem unaltered, although very weak aqueous alteration of GEMS is reported in UCAMM D05IB80 [2], or potential thermal alteration during atmospheric entry for DC060594 [20].

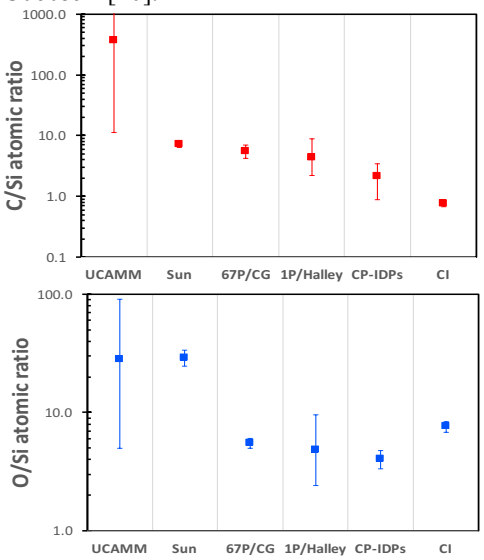


**Figure 2**: C/Si (top) and O/Si (bottom) atomic ratios updated from [21] with data for UCAMMs (this work), the Sun and CI chondrites [22], comet 67P/Churyumov-Gerasimenko [21], comet 1P/Halley [23], and CP-IDPs [24].

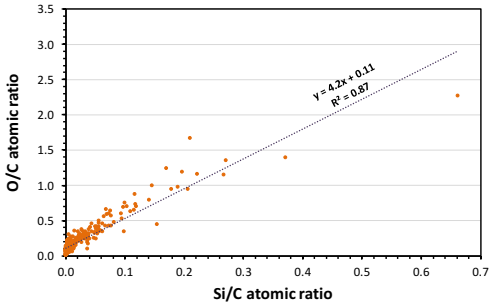


**Figure 3**: EMPA data for 10 UCAMMs showing the correlation of O/C vs. Si/C. The O/Si obtained by regression is ~ 4.

Irradiation tracks are observed in low-Ca pyroxenes in UCAMM DC060443 [8], supporting an origin of these minerals from the inner solar system. Using the track production rate at 1 AU determined by [25], the inferred exposure ages of these pyroxenes are in the order of a few hundred thousand years. However, such exposure ages should be taken with caution as uncertainties remain in the relation between track production rate and exposure ages extrapolated to 4.5 Ga ago.

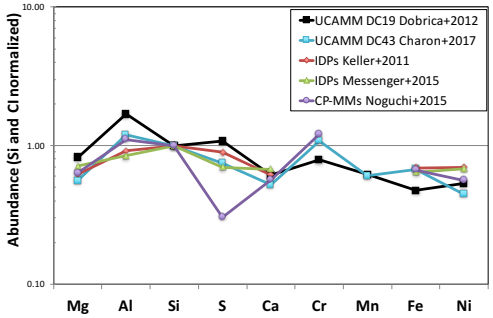


**Figure 4**: Average bulk composition of GEMS in UCAMMs [6, 8], IDPs [26, 27] and CP-AMMs [28].

**Conclusions**: The organic matter of UCAMMs embeds high temperature minerals formed close to the early Sun and GEMS which obviously formed at lower temperature, with an average solar bulk O/Si atomic ratio. Organics adjacent to these minerals have preserved isotopic heterogeneities in both hydrogen and nitrogen elements. The elemental composition of the organic matter shows different phases with a varying N-content, and an O-content lower than in meteoritic IOM. The N/C and C/Si ratios characterizing the UCAMM are higher than the interstellar value, precluding a direct presolar heritage (see also [15]). The N-rich UCAMM organic matter may have been formed by irradiation of ices at the surface of a parent body in the outer regions of the protoplanetary disk [29], mixed with IOM-like organic matter, and with minerals transported by radial mixing from the inner Solar System.

**References:** [1] Nakamura T., *et al.* (2005) *MAPS* **40 Suppl.**, #5046. [2] Yabuta H., *et al.* (2017) *GCA* **214**, 172-190. [3] Noguchi T., *et al.* (2017) *GCA* **208**, 119-144. [4] Dobrică E., *et al.* (2008) *LPSC* **XXXIX**, #1672. [5] Duprat J., *et al.* (2010) *Science* **328**, 742-745. [6] Dobrică E., *et al.* (2012) *GCA* **76**, 68-82. [7] Engrand C., *et al.* (2015) *LPSC* **46**, #1902. [8] Charon E., *et al.* (2017) *LPSC* **48**, #2085. [9] Duprat J., *et al.* (2014) *MAPS* **49 Suppl.**, #5341. [10] Bardin N., *et al.* (2015) *MAPS* **50 Suppl.**, #5275. [11] Briani G., *et al.* (2012) *MAPS Suppl.* **47 Suppl.**, #5362. [12] Briani G., *et al.* (2012) *LPSC* **43**, #2584. [13] Dobrică E., *et al.* (2011) *MAPS* **46**, 1363-1375. [14] Dartois E., *et al.* (2013) *Icarus* **224**, 243-252. [15] Dartois E., *et al.* (2018) *A&A*, in press. [16] Yabuta H., *et al.* (2012) *LPSC* **43**, #2239. [17] Yabuta H., *et al.* (2012) *MAPS Suppl.* **75**, #5196. [18] Bouwman J., *et al.* (2008) *ApJ* **683**, 479. [19] Tushar M., *et al.* (2015) *ApJ* **798**, 87. [20] Bradley J.P. and Ishii H. (2017) *MAPS* **52 Suppl.**, A33 (#6260). [21] Bardyn A., *et al.* (2017) *MNRAS* **469**, S712-S722. [22] Lodders K. (2010) in *Principles and Perspectives in Cosmochemistry*, 379-417. [23] Jessberger E.K., *et al.* (1988) *Nature* **332**, 691-695. [24] Thomas K.L., *et al.* (1993) *GCA* **57**, 1551-1566. [25] Berger E.L. and Keller L.P. (2015) *LPSC* **46**, 1543. [26] Keller L.P. and Messenger S. (2011) *GCA* **75**, 5336-5365. [27] Messenger S., *et al.* (2015) *MAPS* **50**, 1468-1485. [28] Noguchi T., *et al.* (2015) *EPSL* **410**, 1-11. [29] Augé B., *et al.* (2016) *A&A* **592**, A99.